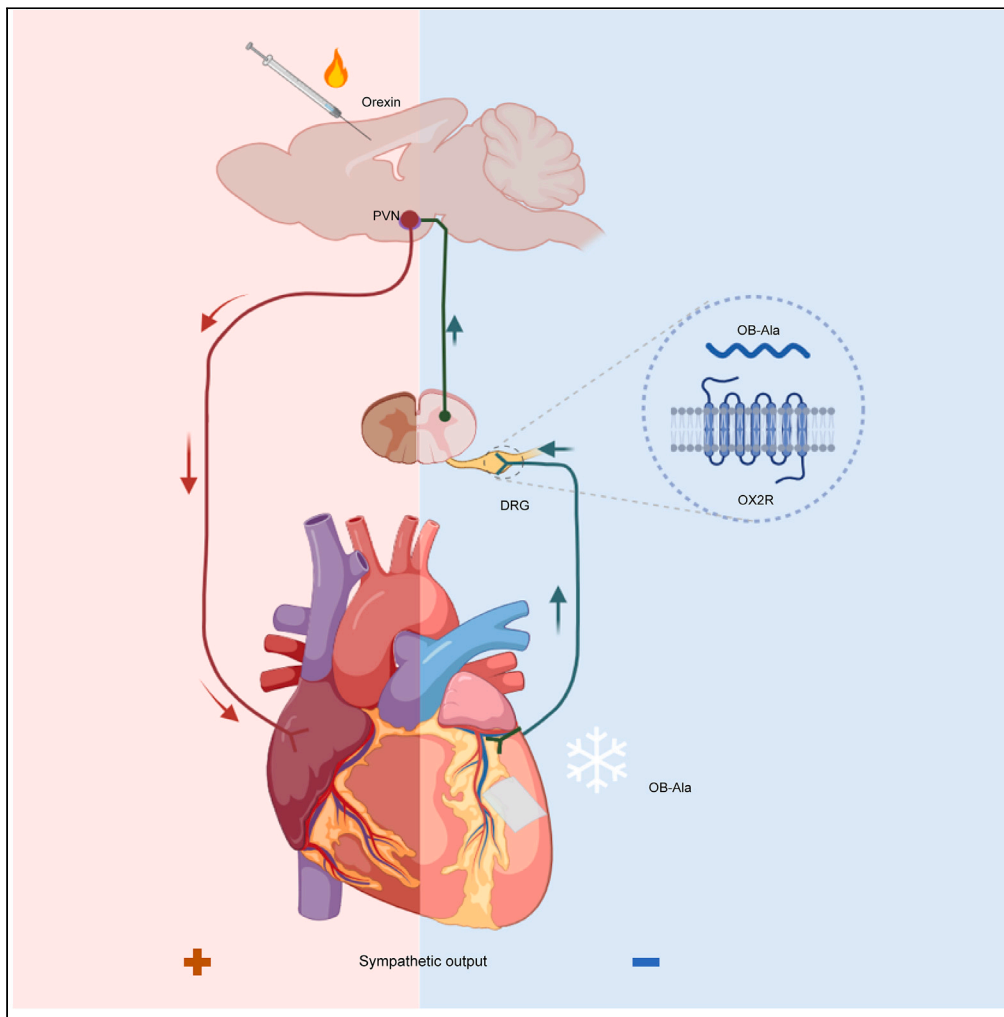**Article**

An orexin-receptor-2-mediated heart-brain axis in cardiac pain

Han Jiao, Yongjin Wang, Kang Fu, ..., Juan Lv, Li Su, Yuanqing Gao

yuanqinggao@njmu.edu.cn

Highlights

OX2R signaling in DRG and hypothalamus has opposite effects in PVN neurons

OX2R is located in primary afferent nerve endings innervating heart

Activation of OX2R in DRG attenuated capsaicin-induced CSAR

OX2R agonists partially rescue acute myocardial infarction

iScience

Article

An orexin-receptor-2-mediated heart-brain axis in cardiac pain

Han Jiao,[1,3,5] Yongjin Wang,[1,5] Kang Fu,[1] Xiaoao Xiao,[1] Mo-Qiu Jia,[1] Jia Sun,[1] Jingxiao Wang,[2] Guoqing Zhu,[2] Daying Lyu,[1] Qiulun Lu,[1] Yu Peng,[1] Juan Lv,[4] Li Su,[4] and Yuanqing Gao[1,6,*]

SUMMARY

Orexin is a neuropeptide released from hypothalamus regulating feeding, sleeping, arousal, and cardiovascular activity. Past research has demonstrated that orexin receptor 2 (OX2R) agonist infusion in the brain results in sympathoexcitatory responses. Here, we found that epicardial administration of OX2R agonism leads to opposite responses. We proved that OX2R is expressed mainly in DRG neurons and transported to sensory nerve endings innervating the heart. In a capsaicin-induced cardiac sympathetic afferent reflex (CSAR) model, we recorded the calcium influx in DRG neurons, measured heart rate variability, and examined the PVN c-Fos activity to prove that epicardial OX2R agonism administration could attenuate capsaicin-induced CSAR. We further showed that OX2R agonism could partially rescue acute myocardial infarction by reducing sympathetic overactivation. Our data indicate that epicardial application of OX2R agonist exerts a cardioprotective effect by attenuating CSAR. This OX2R-mediated heart-brain axis may provide therapeutic targets for acute cardiovascular diseases.

INTRODUCTION

The orexin peptides are important hypothalamic neuropeptide hormones that participate in a wide range of biological activities including feeding, thermogenesis, attention, arousal, glucose metabolism, pain modulation, and cardiovascular activity.[1] Orexin peptides have two subtypes: orexin A (OA) and orexin B (OB). They are derived from a common precursor peptide prepro-orexin (PPO). Orexin-producing neurons are located exclusively in the lateral hypothalamus and supposed to be the only source of orexin peptides.[2] Orexin system exerts its biological actions via orexin receptor 1 (OX1R) and orexin receptor 2 (OX2R), which are widely distributed in the central nervous system and some peripheral tissues.

Orexin signaling was previously reported to regulate cardiovascular activity through both OX1R and OX2R distributed in different brain regions. Central administrated orexin A (OA), which binds to both OX1R and OX2R, could increase heart rate and blood pressure.[3] Microinjection of OA or OB into central autonomic regulation regions like rostral ventrolateral medulla (RVLM) and solitary nucleus (NTS) could also evoke cardiovascular responses, and such effects could be abolished by OX1R and OX2R antagonisms given centrally.[4–6] Meanwhile, orexin neurons have been reported to directly innervate sympathetic preganglionic neurons.[7] Thus, a large body of literature suggests that activation of orexin receptors in the brain enhances cardiovascular activities through increased sympathetic output.

Persistent sympathetic hyperactivity contributes to many cardiovascular diseases like hypertension, heart failure, and myocardial infarction. However, a series of recent clinical and animal studies have suggested that OX2R might be protective in heart failure and myocardial infarction in patients and animal models. One clinical study showed that the circulating OA level is positively correlated with therapeutic outcomes in heart failure patients.[8] A genome-wide association study also pointed out that heart failure patients carrying a minor allele upstream of the gene encoding OX2R were less likely to have improved heart function after treatment. OX2R-deficient mice also developed poor cardiac function upon angiotensin II challenge.[9] Altogether, these findings suggest that OX2R signaling is protective in heart failure, which seems to conflict with the previous notion. Thus, the regulatory mechanism of orexin signaling in cardiovascular diseases needs further exploration.

Orexin receptors are also reported to be expressed in the peripheral, like dorsal root ganglia (DRG), adrenal glands, and bone marrow.[2] Previous studies have pointed out that spinal orexin signaling participated in analgesia and pain modulation.[10] In this study, we found that OX2R is expressed in the DRG afferent neurons innervating the heart. The heart is richly innervated by both afferent and efferent nerves, which are critical for cardiovascular activity regulation. The cell bodies of primary afferent neurons of the heart are located in the dorsal root ganglia
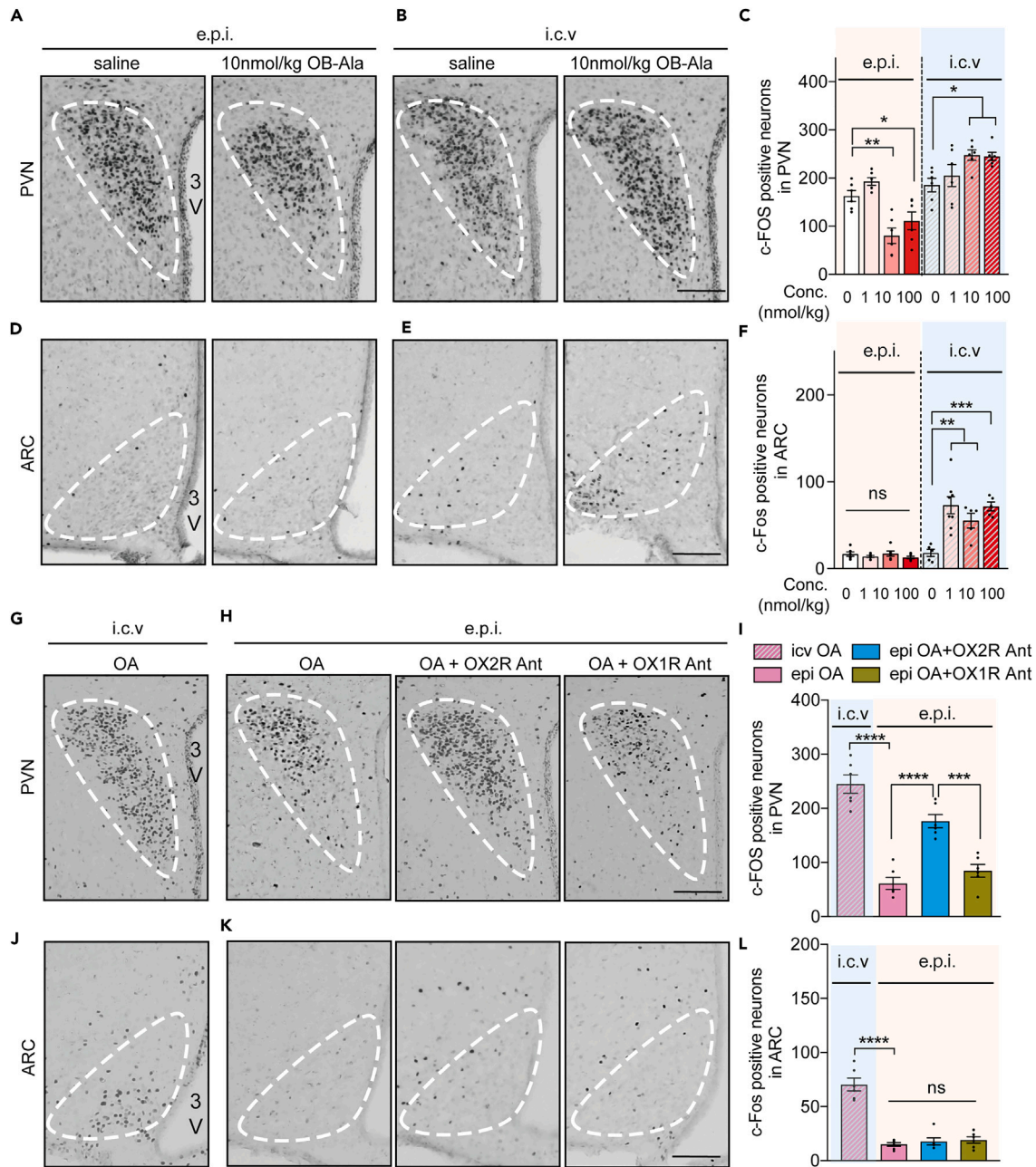
Figure 1. Epicardial application of OX2R agonists attenuates c-Fos activity in PVN

(A) c-Fos staining in PVN 90 min after epicardial application of saline and 10 nmol/kg OB-Ala.

(B) c-Fos staining in PVN 90 min after i.c.v. injection of saline and 10 nmol/kg OB-Ala.

(C) Quantification of c-Fos-positive neuron numbers in PVN 90 min after epicardial application and i.c.v. injection of saline and OB-Ala at 1 nmol/kg, 10 nmol/kg, and 100 nmol/kg.

(D) c-Fos staining in ARC 90 min after epicardial application of saline and 10 nmol/kg OB-Ala.

(E) c-Fos staining in ARC 90 min after i.c.v. injection of saline and 10 nmol/kg OB-Ala.

(F) Quantification of c-Fos-positive neuron numbers in ARC 90 min after epicardial application and i.c.v. injection of saline and OB-Ala at 1 nmol/kg, 10 nmol/kg, and 100 nmol/kg.

(G) c-Fos staining in PVN 90 min after i.c.v. injection of 10 nmol/kg OA.

(H) c-Fos staining in PVN 90 min after epicardial application of OA, OA together with OX2R antagonist or OX1R antagonist.

(I) Quantification of (G) and (H).

Figure 1. Continued

(J) c-Fos staining in ARC 90 min after i.c.v. injection of 10 nmol/kg OA.

(K) c-Fos staining in PVN 90 min after epicardial application of OA, OA together with OX2R antagonist or OX1R antagonist.

(L) Quantification of (J) and (K). N = 6–8 mice per group. Independent experiments were repeated two times. Data are presented as means ± SEM. Significant effect of each dosage by one-way ANOVA. *p < 0.05, **p < 0.01, ***p < 0.001, ****p < 0.0001. Scale bar: 100 μm. PVN, paraventricular nucleus; ARC, arcuate nucleus; OA, orexin A; OX1R, orexin receptor 1; OX2R, orexin receptor 2.

of T2-T6 spinal segments.[11] Cardiac pain could be sensed by cardiac afferent neurons and conveyed to the integration center like the paraventricular nucleus (PVN), thereby triggering a positive feedback loop that enhances sympathetic outflow. This loop is commonly termed cardiac sympathetic afferent reflex (CSAR), which plays an important role in cardiovascular diseases.[12–14] Therefore, we wonder whether OX2R signaling participates in modulating the CSAR responses and cardiovascular activity on cardiac afferent neurons.

In this study, we found that topical application of an OX2R-specific agonist [Ala11, D-Leu15]-OXB (OB-Ala) on the left ventricle reduces c-Fos activation in PVN and heart rate variability (HRV) responses upon capsaicin treatment and attenuated the injury of myocardial infarction. Such effect is mediated through OX2R on cardiac spinal afferent nerves. Thus, the OX2R signaling on afferent neurons inhibits cardiac noxious input and attenuates CSAR, thereby exerting protective effects against acute myocardial infarction. This OX2R-mediated heart-brain-heart loop might shed new light on the drug development strategies for cardiovascular diseases based on the orexin receptor system.

RESULTS

Epicardial application of OX2R agonists attenuate c-Fos activity in PVN

To test whether OX2R signaling in the heart involves the central nervous system, we directly applied 10 nmol/kg OX2R-specific agonist [Ala11, D-Leu15]-OXB (OB-Ala) on the surface of the left ventricle with a small filter paper and checked the c-Fos level in the brain. PVN is known as the central brain region regulating cardiovascular activity. We noticed that in the control group the PVN c-Fos levels are relatively higher than the naive brains, which was probably due to the thoracotomy surgery. Surprisingly, we found OB-Ala application on the heart significantly attenuated the c-Fos activity in PVN (Figure 1A). Because OX2R has been reported to express in PVN neurons, we wondered whether this phenomenon was due to direct cardiac effects or leaking OB-Ala that penetrated into PVN. To clarify this issue, we did an intracerebral ventricle (i.c.v.) injection of OB-Ala with the exact dosage. Mice in both groups were subjected to sham thoracotomy. We found that centrally administrated OB-Ala further promoted c-Fos activity in PVN (Figure 1B). This indicates that the c-Fos reduction in PVN in Figure 1A is a cardiac-specific response upon OB-Ala epicardial treatment. We also tested different doses of OB-Ala and found that 10 nmol/kg and 100 nmol/kg have similar effects, whereas 1 nmol/kg has weaker responses (Figure 1C). Therefore, 10 nmol/kg was employed in the following experiments. The c-Fos activity was also higher in the arcuate nucleus (ARC) with the central administration of OB-Ala and not affected by epicardial OB-Ala application (Figures 1D–1F). The c-Fos activity was not different among groups in the dorsomedial hypothalamus and supraoptic nucleus (Figures S1A–S1F).

To further distinguish the contribution of OX1R and OX2R, we employed endogenous dual agonist Orexin A (OA) together with an OX1R-specific antagonist SB334867 or an OX2R-specific antagonist EMPA. As shown in Figures 1G–1I, c-Fos activity in PVN is similar between OA and OB-Ala when given i.c.v. Epicardial application of OA attenuated c-Fos activity in PVN, which is also similar to OB-Ala effect. Such inhibitory effect could be blocked by OX2R antagonist but not by OX1R antagonist, indicating OX2R is more important in this scenario. In ARC, i.c.v. injection of OA induced an increase in c-Fos level as OB-Ala while epicardial application of OA, OA together with OX2R antagonist or OX1R antagonist, did not trigger obvious responses (Figures 1J–1L). These data further support that OX2R activation in the heart could inhibit PVN neuron activity, opposite to OB-Ala's direct effects on PVN neurons.

OX2R expression in DRG neurons innervating heart

It has been reported that OX2R is expressed in cardiomyocytes.[15] However, this cannot explain the PVN c-Fos reduction upon cardiac OB-Ala application. The Orexin system was also documented to participate in pain regulation in DRG. In the brain of mice that received epicardial OB-Ala treatment, the attenuated c-Fos level was also observed in the periaqueductal gray (PAG) region (Figures S1G–S1L), a key region in the modulation of nociception.[16] Therefore, we speculate that OB-Ala may modulate cardiac pain by spinal afferent fibers innervating the heart. Due to the lack of reliable antibody of OX2R for immunohistochemistry, we performed *in situ* hybridization of *Hcrtr2* in heart and dorsal root ganglia at both organ and cell level by RNAscope kit. *Hcrtr2* mRNA was barely detected in heart tissue (Figure 2A) but abundant in dorsal root ganglia sensory neurons marked by CGRP staining (Figure 2B). qPCR results also confirmed that the mRNA expression level of *Hcrtr2* was relatively high in the dorsal root ganglia and hypothalamus while almost undetectable in the heart (Figure 2C). The protein level profile of OX2R is just opposite to mRNA results. OX2R protein could be detected in the left ventricle and atrium of the heart but not in dorsal root ganglia (Figure 2D). This pattern suggests that OX2R might be transcribed in the cell body of sensory neurons in dorsal root ganglia and transported to the fiber terminals innervating the heart. We then isolated the DRG neurons and seeded them in the culture and found out that DRG neurons express comparable level of OX2R proteins as hypothalamic neurons (Figure 2D). To further confirm this hypothesis, we isolated and cultured mouse primary cardiomyocytes and sensory neurons from DRG *ex vivo* and checked the mRNA expression of *Hcrtr2*. Similarly, mRNA of *Hcrtr2* could be detected by RNAscope and qPCR in sensory neurons but undetectable in neonatal cardiomyocytes (Figures 2E–2G). We also examined the mRNA expression of *Hcrtr1* in tissue and cultured primary cells. Slightly different from the *Hcrtr2*, although *Hcrtr1* also has comparable expression levels in DRG and hypothalamus, it is also detectable in cardiomyocytes and heart tissues (Figures 2H and 2I). Together, these data indicate that OX2R is mainly synthesized in sensory neurons in dorsal root ganglia, and the protein of
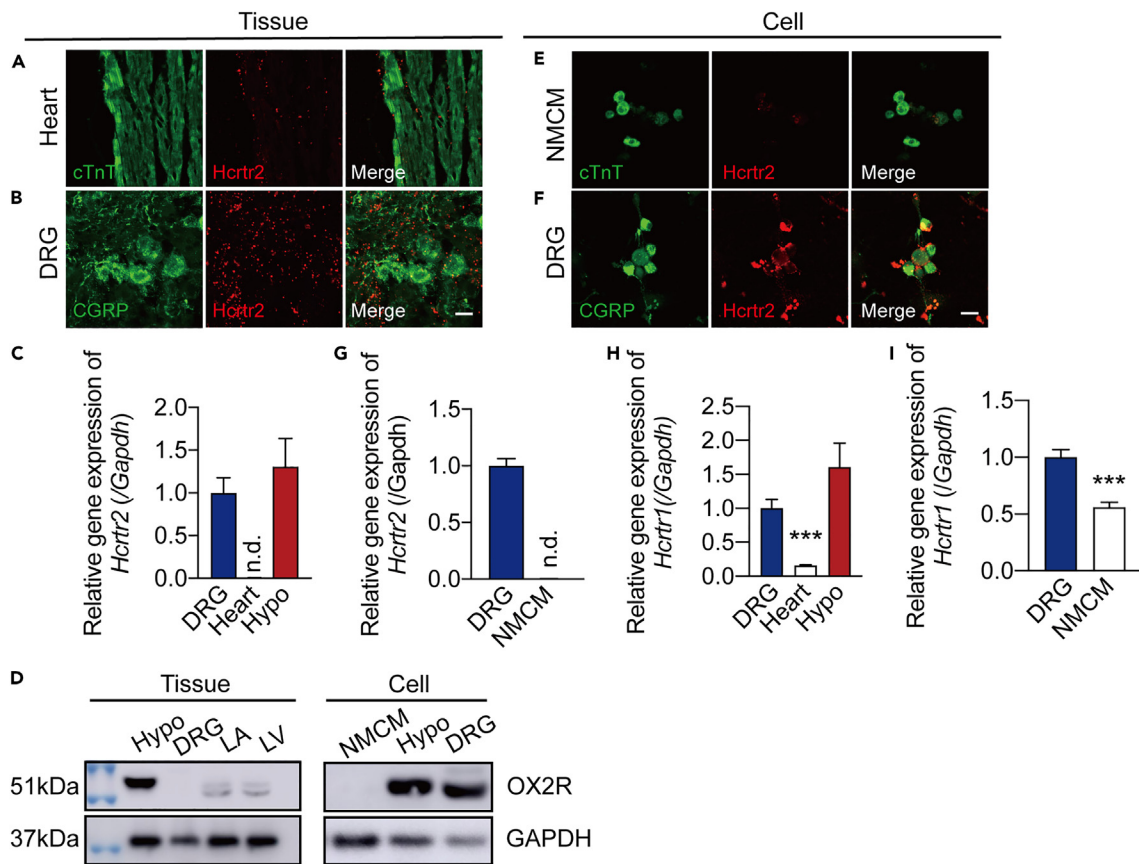
Figure 2. OX2R is mainly expressed in DRG neurons

(A) mRNA of *Hcrtr2* distribution in heart tissue visualized by RNAscope. Cardiomyocytes are labeled by cTnT.

(B) mRNA of *Hcrtr2* distribution in DRG visualized by RNAscope. Sensory neurons in DRG are labeled by CGRP.

(C) mRNA of Hcrtr2 in heart and DRG detected by qPCR. Hypothalamus tissues are used as a positive reference. Tissues were obtained from three animals.

(D) The protein level of OX2R in the heart and DRG tissue or primary culture detected by western blot. LA, left atrium; LV, left ventricle. Hypothalamus tissues and primary cultured hypothalamic neurons are used as a positive reference.

(E) mRNA of *Hcrtr2* in cultured cardiomyocytes (labeled by cTnT) isolated from neonatal mouse (NMCM) detected by RNAscope.

(F) mRNA of *Hcrtr2* in cultured neurons isolated from DRG of the neonatal mouse by RNAscope. Sensory neurons are labeled by CGRP.

(G) mRNA expression of *Hcrtr2* in cultured NMCM and cultured DRG neurons detected by quantitative PCR.

(H) mRNA of *Hcrtr1* in heart, DRG, and hypothalamus detected by quantitative PCR.

(I) mRNA expression of *Hcrtr1* in cultured NMCM and cultured DRG neurons detected by qPCR. Primary DRG neurons were isolated from 15 neonatal mice with 5 technical repeats (5 culture wells). Primary NMCM were isolated from 20 neonatal mice with 5 technical repeats (5 culture wells). All data are presented as means $\pm$ SEM. $*p < 0.05$, $**p < 0.01$, $***p < 0.001$, $****p < 0.0001$. Scale bar: 20 μm.

OX2R detected by western blot in the heart tissue is probably mostly located in sensory nerve endings on the heart surface. Meanwhile, OX1R is expressed in both DRG neurons and cardiomyocytes, indicating a more complicated regulating mechanism involved.

OX2R agonist blocks capsaicin-induced Ca²⁺ flux in DRG

To further confirm the effect of OB-Ala in sensory neurons upon capsaicin stimulation, calcium flux was recorded in sensory DRG neurons in culture. Capsaicin is a classic chemical stimulus to induce nociceptive responses. A notable increase of intracellular calcium flux could be observed in response to capsaicin by Fluo-8 calcium kit under a confocal microscope. Adding OB-Ala or OA together with the capsaicin significantly attenuated the calcium influx. Such inhibitory effect was abolished by the pretreatment of OX2R antagonist but not OX1R antagonist (Figures 3A and 3B), indicating that OB-Ala could indeed decrease the depolarization of the nociceptive neurons in DRG through OX2R upon noxious stimulus.

OX2R agonist inhibits capsaicin-mediated cardiac sympathetic afferent reflex

Capsaicin was known to induce a cardiac sympathetic afferent reflex (CSAR).[17] We next evaluated whether OB-Ala could prevent capsaicin-induced CSAR *in vivo*. Capsaicin or vehicle solvent was dropped on a sterilized filter paper that was applied on the top of the heart together
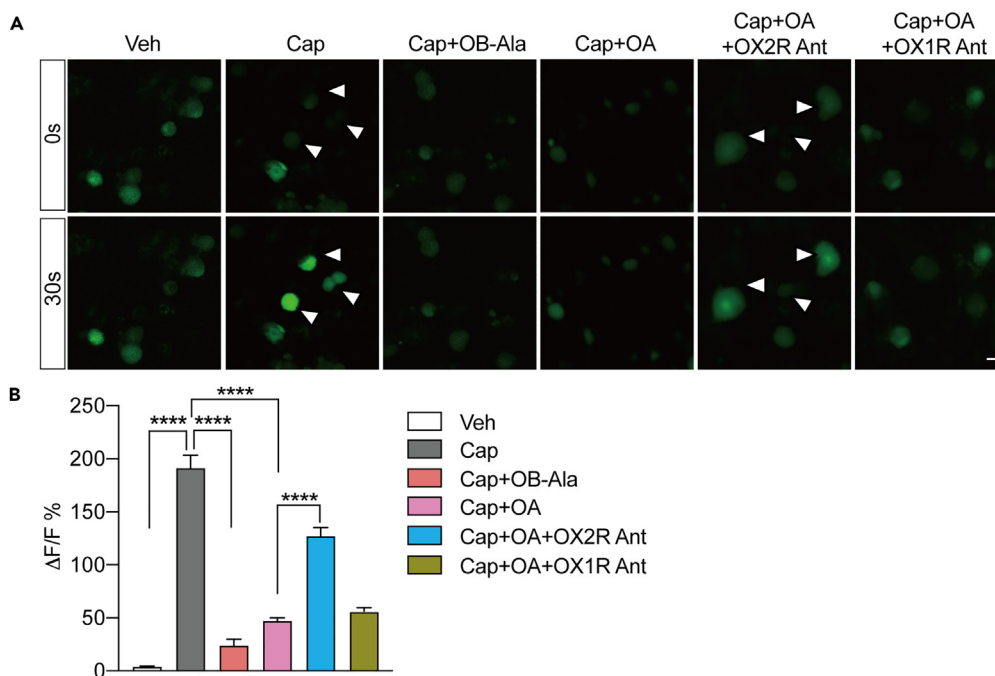
Figure 3. OX2R agonist blocks capsaicin-induced Ca²⁺ flux in DRG

(A) Fluo-8 indicated calcium images of cultured DGR neurons at 0 s and 30 s after Veh, 10 μM capsaicin, capsaicin + OB-Ala, capsaicin + OA, capsaicin + OA + OX2R antagonist, and capsaicin + OA + OX1R antagonist.

(B) Quantification of calcium fluorescent change rate peak (about 30 s) in (A). 17/42/47/34/81/61 cells from five isolations were recorded for (A). Significant effect of each treatment by one-way ANOVA. Data are presented as means ± SEM. ****$p < 0.0001$. Scale bar: 20 μm.

with or without OB-Ala. Lidocaine was employed as a reference drug that was known to inhibit CSAR. PVN and nucleus tractus solitarii (NTS) are important integrative centers of CSAR. We found that the c-Fos level in PVN is elevated by epicardial capsaicin treatment and markedly attenuated by OB-Ala and lidocaine as well (Figures 4A and 4B). The same pattern could be observed in NTS (Figures 4C and 4D) and PAG (Figures 4E and 4F) regions. Meanwhile, no significant changes have been observed among four groups in the dorsal motor nucleus of the vagus. The endogenous dual agonist OA had similar effects as OB-Ala, and such response could be abolished by epicardial pretreatment of OX2R antagonist EMPA but not OX1R antagonist SB334867 (Figures 4G–4L), which further supports a dominant role of OX2R-mediated signaling. To explore which subpopulation of neurons were activated by capsaicin and inhibited by OB-Ala in PVN, we co-stained c-FOS with oxytocin and corticotropin-releasing factor (CRF) (Figure S2). Based on the localization results and anatomical distribution pattern, these responding neurons are perhaps CRF-positive parvocellular pre-sympathetic neurons. Meanwhile, we found the circulating orexin level was elevated after epicardial capsaicin treatment (Figure S3).

To further investigate the role of sensory afferent nerves in this particular phenotype, we repeated the capsaicin experiment on animals in which nociceptive sensory nerves had been ablated. Nociceptive sensory nerve denervation was achieved through resiniferatoxin (RTX) injection and demonstrated by the downregulation of Trpv1 and calcitonin-gene-related peptide (CGRP) mRNA expression in DRG (Figures S4A and S4B). In the control group, capsaicin led to an elevation in c-Fos levels in the PVN, same as Figure 4 (Figures S4C and S4D). This activation was completely abolished in the RTX group, regardless of whether capsaicin or OB-Ala treatment was administered (Figures S4E–S4G). These results provide further evidence supporting the involvement of nociceptive sensory nerves in capsaicin-induced CSAR.

To further assess the effect of OB-Ala in CSAR responses, we analyzed the activity of cardiac autonomic nervous system based on HRV. Due the instability of HRV data in the mouse model, this experiment was performed in rats. Normalized LF values are determined by both sympathetic and parasympathetic activities, but are dominated by sympathetic activities, whereas the normalized HF values mainly indicate the parasympathetic activities. Thus, the LF/HF ratio is an index of sympathetic-parasympathetic balance. We observed that epicardial application of capsaicin induced a classic CSAR response represented by increased LF and LF/HF ratio, whereas the pretreatment of OB-Ala could prevent the capsaicin-induced elevation of LF and LF/HF ratio. Administration of vehicle (corn oil) or OB-Ala alone did not trigger any changes in HRV variables (Figures 5A–5C). Meanwhile, we also measured arterial blood pressure (ABP), mean arterial blood pressure (MAP), and heart rate (HR) after capsaicin stimulus with and without OB-Ala pretreatment. Similar to HRV data, the ABP, MAP, and HR responses evoked by capsaicin were almost completely abolished by the pretreatment of OB-Ala (Figure 5D–5F). Taken together, these results indicate that epicardial treatment of OB-Ala could attenuate the sympathoexcitatory reflex upon capsaicin stimulus.
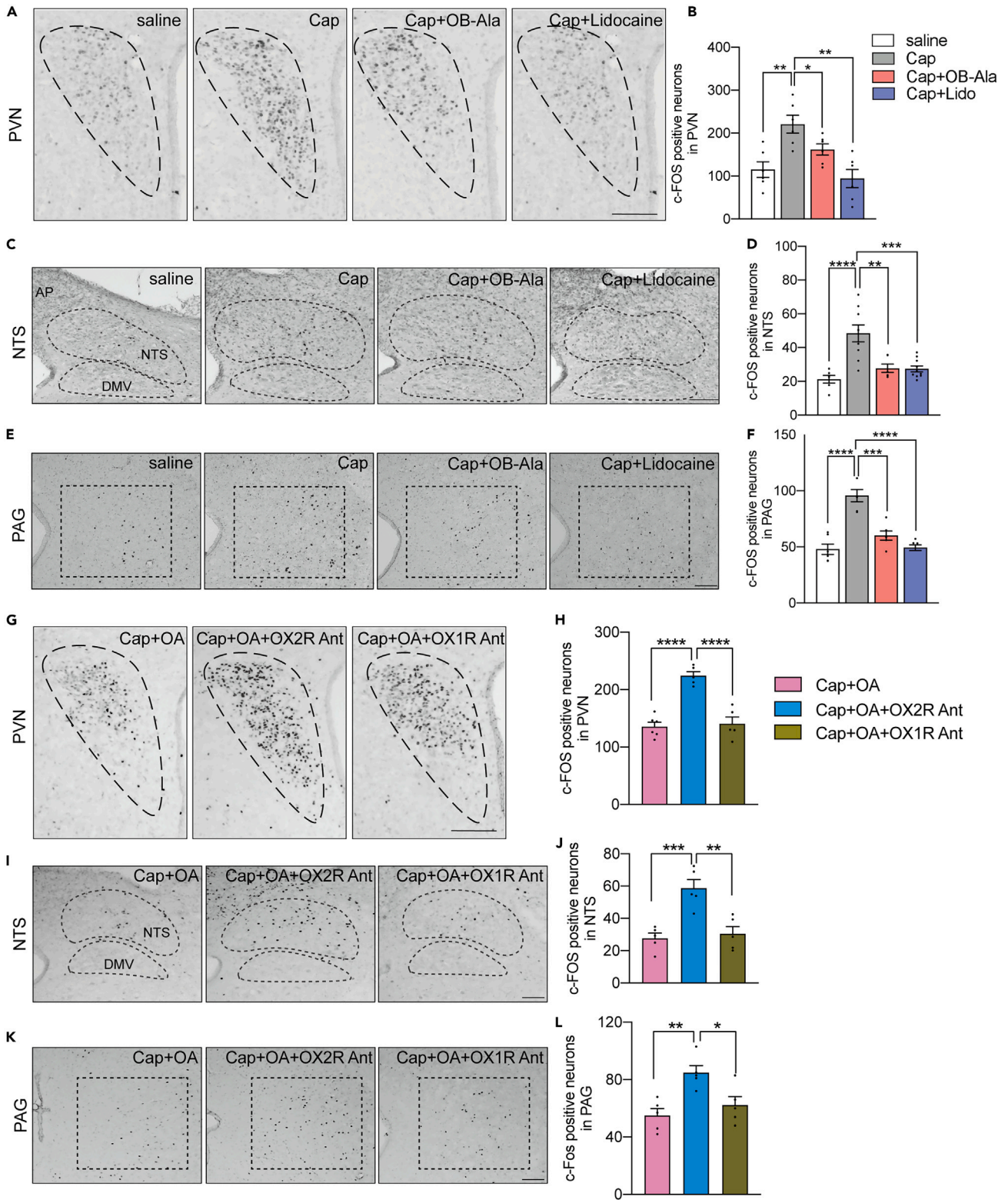
Figure 4. OX2R agonist inhibits c-Fos activity in the nucleus involved in capsaicin-mediated cardiac sympathetic afferent reflex

c-Fos activity in PVN (A and B), NTS (C and D), and PAG (E and F) after epicardial application of saline, capsaicin, capsaicin + OB-Ala, and capsaicin + lidocaine. c-Fos activity in PVN (G and H), NTS (I and J), and PAG (K and L) after epicardial application of capsaicin + OA, capsaicin + OA + OX2R antagonist, and capsaicin OA + OX1R antagonist. N = 6–10 mice per group. Independent experiments were repeated at least two times. Significant effect of each treatment by one-way ANOVA. Data are presented as means ± SEM. *p < 0.05, **p < 0.01, ***p < 0.001, ****p < 0.0001. Scale bar: 100 μm in all panels.

OX2R agonist exerts a protective role in acute myocardial infarction

Enhanced CSAR contributes to acute myocardial infarction, ischemia, and chronic heart failure. Therefore, we next tested whether the epicardial application of OB-Ala could protect the heart against acute myocardial infarction. Acute myocardial infarction was induced by ligation of the left anterior descendant (LAD) coronary artery. Mice in the control group received sham surgery. OB-Ala or saline was applied to the surface of the left ventricle in the same way as the capsaicin experiment. The c-Fos activity was checked in the PVN 90 min after surgery. We found that in the myocardial infarction group the c-Fos level was strongly elevated as reported in the literature, and OB-Ala significantly reduced such activation (Figures 6A and 6B). The same pattern was observed in the PAG region (Figure 6C). Besides, the c-Fos level in the spinal intermediolateral nucleus (IML) where the sympathetic preganglionic neurons are located was also elevated in the LAD surgery group and inhibited by OB-Ala treatment (Figure S5). Heart function was analyzed 24 h later, and tissues were harvested for detailed analysis. In line with PVN c-Fos results, OB-Ala treatment partially rescued LAD-ligation-induced myocardial infarction as indicated by TTC staining (Figures 6D and 6E). Ejection fraction and fractional shortening (Fs) reduction by LAD surgery were also rescued in part by OB-Ala (Figures 6F and 6G). Masson staining also showed that OB-Ala reduced the collagen volume fraction (CVF) induced by LAD ligation (Figures 6H and 6I). Together, these data indicate that epicardial application of OB-Ala could protect the heart from acute infarction injury via attenuating CSAR. Orexin receptors have been reported able to couple with multiple G-proteins including Gq, Gi/o, and Gs, depending on tissues and cell types. To elucidate the mechanism behind OB-Ala-mediated protective effect through OX2R, we measured the cAMP levels in DRGs innervating the heart (T2-T6).[18] As shown in Figure 6J, cAMP levels were elevated in DRGs from mice with myocardial infarction and decreased by epicardial treatment of OB-Ala, which indicated an OX2R-Gi coupling upon OB-Ala stimulation, leading to inhibition of cAMP synthesis.

DISCUSSION

In this study, we showed that the epicardial application of a specific OX2R agonist could protect the heart from myocardial infarction injury. The protective effect is due to the reduction of cardiac sympathetic afferent reflex that is mediated by OX2Rs distributed on sympathetic afferent nerve endings that innervate the heart.

Here, we found that topical administration of OX2R agonist on the heart has inhibitory effects on PVN c-Fos activity. This effect is just opposite to i.c.v. injection responses. Therefore, we can confirm that epicardial activation of OX2R triggers a distinct response in PVN. PVN is the coordinative center of CSAR, containing pre-sympathetic neurons that project to RVLM and IML.[19] We also observed the reduction of c-Fos level in IML in OB-Ala-treated MI mice. These data in mice are also consistent with the HRV data in rats. LF, LF/HF ratio, MBP, and HR responses caused by capsaicin could be abolished by OX2R agonist pretreatment. All these data indicate a decreased sympathetic outflow upon epicardial OX2R activation. Although vagus nerves are also important for cardiovascular activity regulation, there were no observable changes in vagus nerves in our study. Evidence from screening study of all the GPCRs in vagal Nav1.8-expressing afferents does not support the existence of orexin receptors in vagal afferent neurons.[20] The c-Fos signal was not detected in the dorsal motor nucleus of the vagus in any groups. In HRV experiments, the HF values, which mainly represent the parasympathetic activities, have not differed among groups either. Thus, we believe that the vagus nerve is less relevant in this work. Also, it is worthwhile to be mentioned that the HRV study was done on anesthetized animals that may not fully mimic the physiological situation.

Orexin receptors have been reported to be expressed in the brain and peripheral tissues as well. A recent study pointed out an important role of OX1R on pre-neutrophils in protecting mice against atherosclerosis with fragmented sleep.[2] We provided evidence that although OX2R protein could be detected in heart tissue, the mRNA level of OX2R is much lower than DRG. Also, in isolated primary cells, the mRNA level of OX2R in cardiomyocytes is much lower than in cultured ganglions. This pattern is common for some neurotransmitter transporters and sensory receptors that are synthesized in afferent neuron cell bodies and translocated to the nerve endings to execute the function. For instance, capsaicin and bradykinin are well-established pain mediators that enhance CSAR via TRPV1 receptor and BA receptor, respectively, on afferent neurons terminals.[21] Therefore, we propose that OB-Ala works in the same way via OX2R on afferent nerve endings to participate in CSAR responses.

Our findings are also in line with the analgesic effect of orexins. OXA has been proved to have antinociceptive effects at spinal and supraspinal levels.[10] OXA and OX1R agonists show analgesic effects in various kinds of pain like neuropathic pain, visceral pain, headache, etc. Most of these studies used OXA, which is a dual agonist for both OX receptors. The rest of the studies focused on OX1R by using an OX1R agonist SB334867. The role of OX2R in pain modulation has not been evaluated sufficiently. A series of recent genetics association studies pointed out the link between *Hcrtr2* SNP variants and cluster headache, whereas the detailed mechanism remains unclear.[22] In the current study, we provided evidence that OX2R agonist could directly inhibit capsaicin-induced nociceptive responses both *in vivo* and *ex vivo*. We also employed the dual agonist OA combined with OX1R and OX2R antagonist, respectively, to prove the critical role of OX2R over OX1R behind this protective effect, suggesting an anti-nociceptive effect of OB-Ala via OX2R specifically.

Cardiac pain could be conveyed to the central by both chemosensitive nociceptors and mechanoreceptors. Chemical mediators like capsaicin, bradykinin, and substance P could directly activate cardiac afferent C fibers and induce a sympathetic reflex. This positive
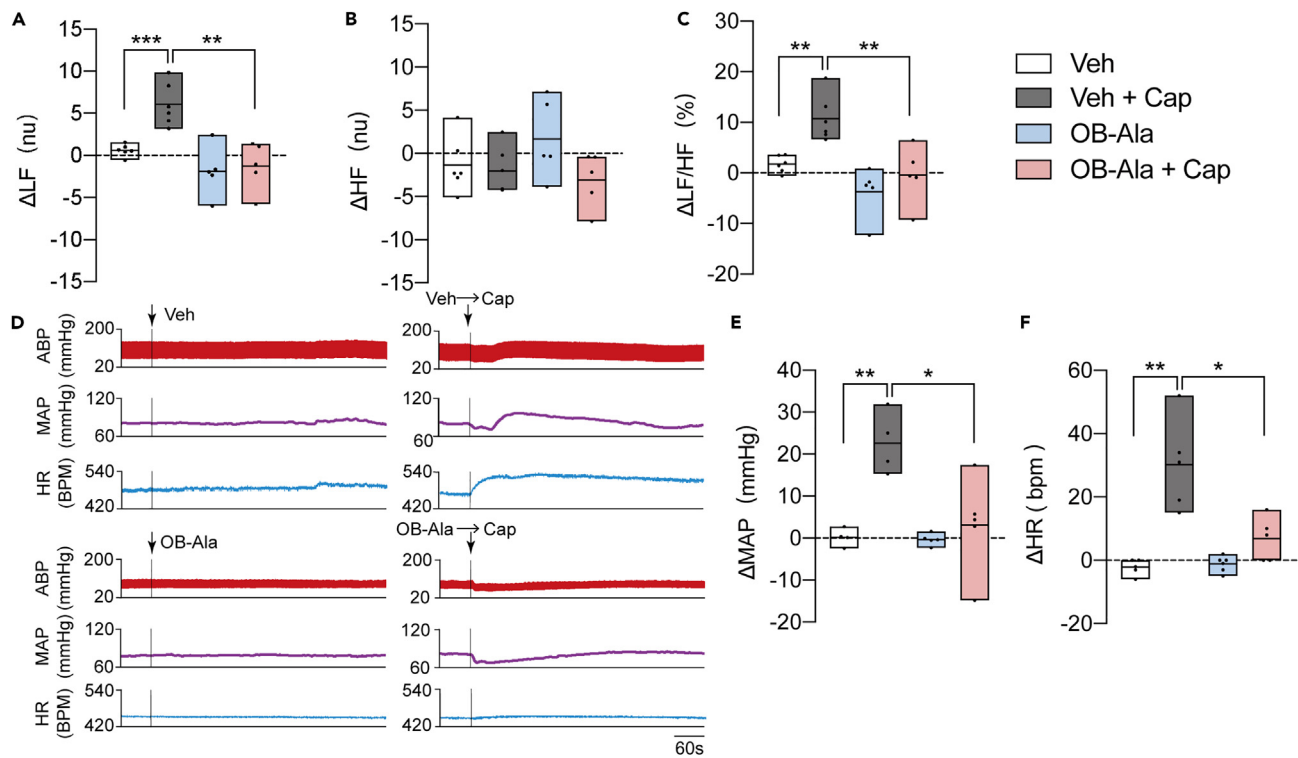
Figure 5. OX2R agonist inhibits capsaicin-induced sympathoexcitatory responses on HRV, MAP, and HR

Rats received epicardial capsaicin with and without OB-Ala pretreatment.

(A–C) The changes in HRV were indicated by the changes of LF (A), the changes of HF (B), and the relative changes of LF/HF (C).

(D) Representative original tracing of ABP, MAP, and HR in four groups.

(E) Quantification of maximum change of MAP within 2 min after every intervention.

(F) Quantification of maximum change of HR within 2 min after every intervention. N = 5–6 per group. Significant effect of each treatment by one-way ANOVA. Data are presented as means ± SEM. *p < 0.05, **p < 0.01, ***p < 0.001. Scale bar: 60 s in (D).

feedback loop of sympathetic outflow has been reported in chronic heart failure, myocardial infarction, and hypertension across the species.[23] Blocking this positive sympathetic loop is an important therapeutic strategy in cardiovascular diseases.[17] In this study, we reported that OB-Ala might work as a potential analgesic drug to inhibit cardiac pain transmission and in turn to attenuate CSAR via the OX2R receptor and thereby protect the heart from sympathetic overactivity. In another study, OB-Ala was reported to exert a protective function in *ex vivo* isolated hearts without extrinsic innervation.[15] We speculate that such effects might be mediated through intrinsic cardiac ganglion, which is also a part of the cardiac autonomic nervous system. Thus, whether intrinsic cardiac ganglion has functional OX2R needs further exploration.

We demonstrated here the pharmacological activation of OX2R has the opposite effect on PVN c-Fos activity and perhaps also the sympathetic outflow, whereas the physiological situation is more complicated. A few studies reported that the orexin could be synthesized from the adrenal cortex, cardiomyocytes, and enteric neurons[15,24,25]; however, these findings have not been corroborated by other studies. The orexin neurons in the later hypothalamus are still assumed to be the major source of circulating orexins. A higher circulating OXA level is associated with better therapeutic outcomes in heart failure patients,[8] suggesting that endogenous OXA may be a beneficial prognostic marker. We also found that circulating orexin level is higher upon epicardial capsaicin treatment. Thus, whether a similar feedback regulatory loop exists for the endogenous orexin system during pathological situation needs further exploration.

Both OX1R and OX2R are GPCRs, and the downstream signaling pathways are dependent on the G-protein-coupling characteristics. In the literature, most of the mechanistic studies focused on the OX1R and demonstrated that activation of OX1R triggers intracellular Ca^{2+} release via Gq-PLC/PLA/PLD pathways.[26,27] A few studies mentioned that OX2R could also couple to Gi proteins in cultured cortical neurons to inhibit cAMP formation.[18] In our study, OB-Ala prevents capsaicin-induced Ca^{2+} increase in DRG neurons and inhibits the cAMP formation upon myocardial infarction, suggesting an OX2R-Gi-coupled downstream cascade in DRG.

Limitations of study and future directions

In this study, we propose that the OX2R-mediated heart-brain axis exerts a significant protective effect under conditions of acute stress or other sympathetic overactivation. However, our research has several limitations. Firstly, due to the absence of DRG neurons in specific
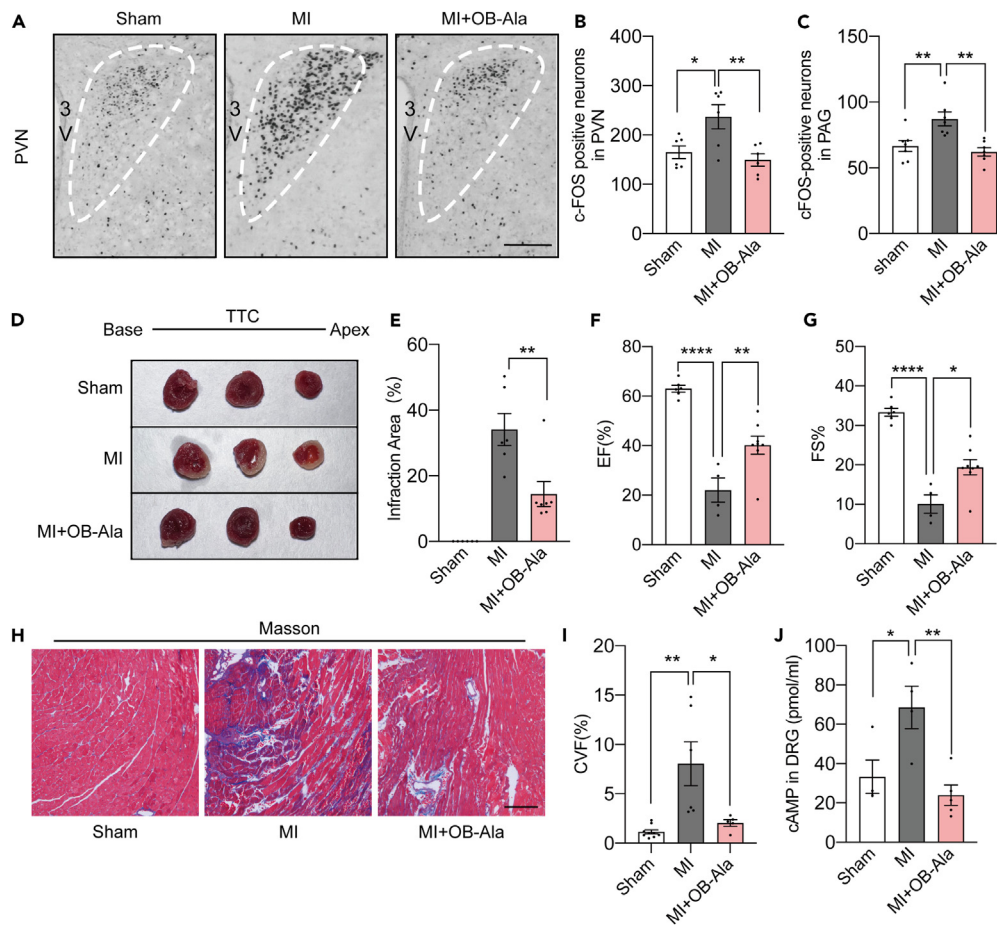
Figure 6. OX2R agonist exerts a protective role in acute myocardial infarction

(A) c-Fos activity in PVN 90 min after LAD ligation surgery with epicardial application of saline or OB-Ala. Quantification of c-Fos-positive neuron numbers in PVN (B) and PAG (C). N = 6–7 mice per group for (A–C). Independent experiments were repeated at least two times.

(D) TTC staining showed infarction area from base to apex of hearts from mice that received sham or LAD ligation surgery with and without OB-Ala.

(E) Quantification of infarction area in (D). Six to seven hearts were analyzed for each group in TTC assay.

(F) Ejection fraction value and (G) fractional shortening value of heart from mice that received sham or LAD ligation surgery with and without OB-Ala 24h after surgery, measured by echocardiography. N = 4–8 per group for (F and G).

(H) Histological section of myocardial tissues from mice with sham or LAD ligation with and without OB-Ala evaluated by Masson staining.

(I) Collagen volume fraction quantification of (H). Five to nine hearts per group were embedded and analyzed for (H and I).

(J) cAMP levels in thoracic DRG from mice that received sham or LAD ligation surgery with and without OB-Ala. N = 4–5 for (J); 10 DRGs (T2-T6) from each animal were collected for each measurement. Significant effect of each treatment by one-way ANOVA for (A–I). Data are presented as means ± SEM. *p < 0.05, **p < 0.01, ***p < 0.001, ****p < 0.0001. Scale bar: 100 μm in (A), 500 μm in (H).

OX2R knockout animals, we tested our hypothesis using pharmacological approaches and sensory nerve denervation methods. Given the complexity of the sympathetic afferent feedback loop, we cannot rule out the possibility that OX2R is expressed in sympathetic nerve endings and participates in peripheral negative feedback effects. Additionally, we cannot entirely dismiss the potential effects of OB-Ala through other tissues and cells expressing OX2R. Another limitation arises from the technical inability to record sympathetic electrophysiological activity in awake states. Our HRV experiments were conducted under anesthesia in rats, which might differ from actual physiological conditions. Furthermore, due to limitations in our drug delivery strategy, we could only apply OB-Ala to the heart surface for a short period and evaluated cardiac function 24 h post-intervention, which is still an early stage for myocardial infarction. Whether this intervention can prevent long-term myocardial infarction injury remains unknown. Currently, there are two dual orexin-receptor antagonists (Suvorexant and Lemborexant) approved for the treatment of insomnia.[28,29] So far, safety studies have reported no major cardiovascular side effects. However, most safety data are limited to healthy subjects. Our data indicate that under acute stress or other sympathetic overactivated condition, cardiac OX2R signaling plays a protective role. Therefore, the cardiovascular safety of these orexin antagonists in patients with cardiovascular diseases still needs further assessment.

STAR★METHODS

Detailed methods are provided in the online version of this paper and include the following:

- KEY RESOURCES TABLE
- RESOURCE AVAILABILITY
  - Lead contact
  - Materials availability
  - Data and code availability
- EXPERIMENTAL MODEL AND STUDY PARTICIPANT DETAILS
  - Animal
- METHOD DETAILS
  - Primary culture
  - Surgery
  - Echocardiography and Doppler imaging
  - Intracerebroventricular injection
  - Measurement of HRV, arterial pressure and heart rate
  - RTX injection
  - Immunohistochemistry and immunofluorescence
  - Western blotting
  - RNAscope *in situ* hybridization
  - Intracellular Ca^{2+} flux assays
  - Measurement of cAMP
  - Image analysis
- QUANTIFICATION AND STATISTICAL ANALYSIS

SUPPLEMENTAL INFORMATION

Supplemental information can be found online at https://doi.org/10.1016/j.isci.2024.109067.

AUTHOR CONTRIBUTIONS

H.J. and Y.G. set up the experiments. H.J., K.F., M.Q.J., and Y.J.W. performed most of the *in vivo* experiments. H.J., M.Q.J., Y.J.W., and J.S. performed *in vitro* experiments and analysis. K.F., Y.J.W., and X.A.X. quantified histology data. K.F. and J.X.W. performed ECG experiments. K.F. and D.L. performed the myocardial surgeries. G.Q.Z. and Q.L. supervised the myocardial infarction surgery and ECG measurement. Y.P., H.J., and J.L. performed the data analysis. H.J., K.F., Y.P., L.S., and Y.G wrote the manuscript. Y.G. conceived the idea and the experimental design. All authors discussed the results and commented on the manuscript.

DECLARATION OF INTERESTS

The authors declare no competing interests.

REFERENCES

1. Carrive, P., and Kuwaki, T. (2017). Orexin and Central Modulation of Cardiovascular and Respiratory Function. Curr. Top. Behav. Neurosci. *33*, 157–196. https://doi.org/10.1007/7854_2016_46.

2. McAlpine, C.S., Kiss, M.G., Rattik, S., He, S., Vassalli, A., Valet, C., Anzai, A., Chan, C.T., Mindur, J.E., Kahles, F., et al. (2019). Sleep modulates haematopoiesis and protects against atherosclerosis. Nature *566*, 383–387. https://doi.org/10.1038/s41586-019-0948-2.

3. Shirasaka, T., Nakazato, M., Matsukura, S., Takasaki, M., and Kannan, H. (1999). Sympathetic and cardiovascular actions of orexins in conscious rats. Am. J. Physiol. *277*, R1780–R1785. https://doi.org/10.1152/ajpregu.1999.277.6.R1780.

4. Shahid, I.Z., Rahman, A.A., and Pilowsky, P.M. (2012). Orexin A in rat rostral ventrolateral medulla is pressor, sympatho-excitatory, increases barosensitivity and attenuates the somato-sympathetic reflex. Br. J. Pharmacol. *165*,

2292–2303. https://doi.org/10.1111/j.1476-5381.2011.01694.x.

5. Samson, W.K., Gosnell, B., Chang, J.K., Resch, Z.T., and Murphy, T.C. (1999). Cardiovascular regulatory actions of the hypocretins in brain. Brain Res. *831*, 248–253. https://doi.org/10.1016/s0006-8993(99)01457-2.

6. Hirota, K., Kushikata, T., Kudo, M., Kudo, T., Smart, D., and Matsuki, A. (2003). Effects of central hypocretin-1 administration on hemodynamic responses in young-adult and middle-aged rats. Brain Res. *981*, 143–150. https://doi.org/10.1016/s0006-8993(03)03002-6.

7. Llewellyn-Smith, I.J., Martin, C.L., Marcus, J.N., Yanagisawa, M., Minson, J.B., and Scammell, T.E. (2003). Orexin-immunoreactive inputs to rat sympathetic preganglionic neurons. Neurosci. Lett. *351*, 115–119. https://doi.org/10.1016/s0304-3940(03)00770-5.

8. Ibrahim, N.E., Rabideau, D.J., Gaggin, H.K., Belcher, A.M., Conrad, M.J., Jarolim, P., and Januzzi, J.L., Jr. (2016). Circulating Concentrations of Orexin A Predict Left Ventricular Myocardial Remodeling. J. Am. Coll. Cardiol. *68*, 2238–2240. https://doi.org/10.1016/j.jacc.2016.08.049.

9. Perez, M.V., Pavlovic, A., Shang, C., Wheeler, M.T., Miller, C.L., Liu, J., Dewey, F.E., Pan, S., Thanaporn, P.K., Absher, D., et al. (2015). Systems Genomics Identifies a Key Role for Hypocretin/Orexin Receptor-2 in Human Heart Failure. J. Am. Coll. Cardiol. *66*, 2522–2533. https://doi.org/10.1016/j.jacc.2015.09.061.

10. Razavi, B.M., and Hosseinzadeh, H. (2017). A review of the role of orexin system in pain modulation. Biomed. Pharmacother. *90*, 187–193. https://doi.org/10.1016/j.biopha.2017.03.053.

11. Gao, J., Zhang, F., Sun, H.J., Liu, T.Y., Ding, L., Kang, Y.M., Zhu, G.Q., and Zhou, Y.B. (2014). Transneuronal tracing of central autonomic regions involved in cardiac sympathetic afferent reflex in rats. J. Neurol. Sci. *342*, 45–51. https://doi.org/10.1016/j.jns.2014.04.023.

12. Chen, W.W., Xiong, X.Q., Chen, Q., Li, Y.H., Kang, Y.M., and Zhu, G.Q. (2015). Cardiac sympathetic afferent reflex and its implications for sympathetic activation in chronic heart failure and hypertension. Acta Physiol. *213*, 778–794. https://doi.org/10.1111/apha.12447.

13. Longhurst, J.C., Tjen-A-Looi, S.C., and Fu, L.W. (2001). Cardiac sympathetic afferent activation provoked by myocardial ischemia and reperfusion. Mechanisms and reflexes. Ann. N. Y. Acad. Sci. *940*, 74–95. https://doi.org/10.1111/j.1749-6632.2001.tb03668.x.

14. Xu, B., Zheng, H., and Patel, K.P. (2013). Relative contributions of the thalamus and the paraventricular nucleus of the hypothalamus to the cardiac sympathetic afferent reflex. Am. J. Physiol. Regul. Integr. Comp. Physiol. *305*, R50–R59. https://doi.org/10.1152/ajpregu.00004.2013.

15. Patel, V.H., Karteris, E., Chen, J., Kyrou, I., Mattu, H.S., Dimitriadis, G.K., Rodrigo, G., Antoniades, C., Antonopoulos, A., Tan, B.K., et al. (2018). Functional cardiac orexin receptors: role of orexin-B/orexin 2 receptor in myocardial protection. Clin. Sci. *132*, 2547–2564. https://doi.org/10.1042/CS20180150.

16. Benarroch, E.E. (2006). Pain-autonomic interactions. Neurol. Sci. *27* (*Suppl 2*), S130–S133. https://doi.org/10.1007/s10072-006-0587-x.

17. Wang, H.J., Wang, W., Cornish, K.G., Rozanski, G.J., and Zucker, I.H. (2014). Cardiac sympathetic afferent denervation attenuates cardiac remodeling and improves cardiovascular dysfunction in rats with heart failure. Hypertension *64*, 745–755. https://doi.org/10.1161/HYPERTENSIONAHA.114.03699.

18. Urbańska, A., Sokołowska, P., Woldan-Tambor, A., Biegańska, K., Brix, B., Jöhren, O., Namieciński, M., and Zawilska, J.B. (2012). Orexins/hypocretins acting at Gi protein-coupled OX 2 receptors inhibit cyclic AMP synthesis in the primary neuronal cultures. J. Mol. Neurosci. *46*, 10–17. https://doi.org/10.1007/s12031-011-9526-2.

19. Pyner, S., and Coote, J.H. (2000). Identification of branching paraventricular neurons of the hypothalamus that project to the rostroventrolateral medulla and spinal cord. Neuroscience *100*, 549–556. https://doi.org/10.1016/s0306-4522(00)00283-9.

20. Egerod, K.L., Petersen, N., Timshel, P.N., Rekling, J.C., Wang, Y., Liu, Q., Schwartz, T.W., and Gautron, L. (2018). Profiling of G protein-coupled receptors in vagal afferents reveals novel gut-to-brain sensing mechanisms. Mol. Metabol. *12*, 62–75. https://doi.org/10.1016/j.molmet.2018.03.016.

21. Zhang, L., Xiong, X.Q., Fan, Z.D., Gan, X.B., Gao, X.Y., and Zhu, G.Q. (2012). Involvement of enhanced cardiac sympathetic afferent reflex in sympathetic activation in early stage of diabetes. J. Appl. Physiol. *113*, 47–55. https://doi.org/10.1152/japplphysiol.01228.2011.

22. Baumber, L., Sjöstrand, C., Leone, M., Harty, H., Bussone, G., Hillert, J., Trembath, R.C., and Russell, M.B. (2006). A genome-wide scan and HCRTR2 candidate gene analysis in a European cluster headache cohort. Neurology *66*, 1888–1893. https://doi.org/10.1212/01.wnl.0000219765.95038.d7.

23. Wang, H.J., Rozanski, G.J., and Zucker, I.H. (2017). Cardiac sympathetic afferent reflex control of cardiac function in normal and chronic heart failure states. J. Physiol. *595*, 2519–2534. https://doi.org/10.1113/JP273764.

24. Lo Pez, M., Sen Aris, R., Gallego, R., Garci A-Caballero, T., Lago, F., Seoane, L., Casanueva, F., and Die Guez, C. (1999). Orexin Receptors Are Expressed in the Adrenal Medulla of the Rat. Endocrinology *140*, 5991–5994. https://doi.org/10.1210/endo.140.12.7287.

25. Kirchgessner, A.L., and Liu, M. (1999). Orexin synthesis and response in the gut. Neuron *24*, 941–951. https://doi.org/10.1016/s0896-6273(00)81041-7.

26. Wang, C., Wang, Q., Ji, B., Pan, Y., Xu, C., Cheng, B., Bai, B., and Chen, J. (2018). The Orexin/Receptor System: Molecular Mechanism and Therapeutic Potential for Neurological Diseases. Front. Mol. Neurosci. *11*, 220. https://doi.org/10.3389/fnmol.2018.00220.

27. Kukkonen, J.P., and Leonard, C.S. (2014). Orexin/hypocretin receptor signalling cascades. Br. J. Pharmacol. *171*, 314–331. https://doi.org/10.1111/bph.12324.

28. Herring, W.J., Snyder, E., Budd, K., Hutzelmann, J., Snavely, D., Liu, K., Lines, C., Roth, T., and Michelson, D. (2012). Orexin receptor antagonism for treatment of insomnia: a randomized clinical trial of suvorexant. Neurology *79*, 2265–2274. https://doi.org/10.1212/WNL.0b013e31827688ee.

29. Murphy, P., Moline, M., Mayleben, D., Rosenberg, R., Zammit, G., Pinner, K., Dhadda, S., Hong, Q., Giorgi, L., and Satlin, A. (2017). Lemborexant, A Dual Orexin Receptor Antagonist (DORA) for the Treatment of Insomnia Disorder: Results From a Bayesian, Adaptive, Randomized, Double-Blind, Placebo-Controlled Study. J. Clin. Sleep Med. *13*, 1289–1299. https://doi.org/10.5664/jcsm.6800.

STAR★METHODS

KEY RESOURCES TABLE

REAGENT or RESOURCE	SOURCE	IDENTIFIER
Antibodies		
Rabbit monoclonal anti-c-Fos(9F6)	Cell Signaling Technology	Cat# 2250T; PRID: AB_2247211
Rabbit anti-CRF	ImmunoStar	Cat# 20084; PRID: AB_10718517
Mouse monoclonal anti-cTnT	Abcam	Cat# ab8295; RRID: AB_306445
Mouse monoclonal anti-CGRP	Abcam	Cat# ab81887; RRID: AB_1658411
Rabbit polyclonal anti-OX2R	Abcam	Cat# ab183072; PRID: N/A
Rabbit anti-GAPDH	Affinity Biosciences	Cat# AF0911; RRID: AB_2839422
Goat Anti-Mouse IgG (H+L) Alexa Fluor 488 conjugated	Jackson ImmunoResearch	Cat# 115-545-003; RRID: AB_2338840
Chemicals, peptides, and recombinant proteins		
Trypsin	Gibco	Cat# 27250018
DMEM	Gibco	Cat# C11995500BT
FBS	Gibco	Cat# 10099141
Penicillin-Streptomycin	Gibco	Cat# 15140122
Type II Collagenase	Yeasen	Cat# 40508ES60
Type II dispase	Yeasen	Cat# 40104ES80
NGF	Gibco	Cat# 13257-019
Isoflurane	RWD	Cat# R510-22
Capsaicin	MCE	Cat# HY-10448
OB-Ala	Tocris	Cat# No.2142
SB334867	MCE	Cat# HY-10895A
EMPA	Sigma	Cat# SML0864
Zoletil	Virbac	Cat# Zoletil 50
Xylazine hydrochloride	MCE	Cat# HY-B0443A
RTX	MCE	Cat# HY-18986
Tissue-Tek® O.C.T. Compound	Sakura	Cat# 4583
IBMX	Aladin	Cat#I106812
Critical commercial assays		
RNAscope 2.5 HD Assay-Red	Advanced Cell Diagnostics	Cat# 322360
Fluo-8 No Wash Calcium Assay kit	Abcam	Cat# ab112129
Cyclic AMP ELISA Kit	Cayman Chemical	Cat# 581001
Experimental models: Organisms/strains		
Mouse: C57BL/6	Animal Core Facility of Nanjing Medical University	N/A
Rat: Sprague Dawley	Animal Core Facility of Nanjing Medical University	N/A
Oligonucleotides		
RNAscope Probe-Mm-Hcrtr2	Advanced Cell Diagnostics	Cat# 460881
Taqman probe *Hcrtr2*	Thermo Fisher	Mm_01179307
Taqman probe *Hprt*	Thermo Fisher	Mm_00446968
Software and algorithms		
GraphPad Prism	GraphPad	https://www.graphpad.com/
ImageJ	(Schneider et al., 2012)	https://imagej.nih.gov/ij/

Continued

REAGENT or RESOURCE	SOURCE	IDENTIFIER
Adobe illustration 14	Adobe	https://www.adobe.com/
LSM800	Leica	https://www2.leicabiosystems.com/
The PowerLab/8SP	ADInstruments	https://m-cdn.adinstruments.com/

RESOURCE AVAILABILITY

Lead contact

Further information and requests for resources and reagents should be directed to the lead contact, Yuanqing Gao (yuanqinggao@njmu.edu.cn).

Materials availability

This study did not generate new unique reagents.

Data and code availability

Data: All data reported in this paper will be shared by the lead contact upon request.

Code: Not applicable.

Any additional information required to reanalyze the data reported in this paper is available from the lead contact upon request.

EXPERIMENTAL MODEL AND STUDY PARTICIPANT DETAILS

Animal

The experimental model employed in this study comprised male C57BL/6 mice, aged 8-10 weeks, and Sprague–Dawley rats with a weight range of 250-300 g. The animals were housed in a controlled environment with a 12-hour light/dark cycle and provided a standard normal diet. Ethical approval for all experiments and protocols was obtained from the Animal Core Facility of Nanjing Medical University under the approval numbers IACUC-1811025 and 2006028.

METHOD DETAILS

Primary culture

For neonatal cardiomyocytes, C57BL/6 mice aged 1 to 3 days were euthanized by decapitation. Hearts were removed immediately. The ventricles were separated from the atria, trisected, and digested with 0.125% trypsin (Gibco, Cat# 27250018) at 37°C for 7 to 10 cycles until completely digested. All supernatants from each cycle except the first were pooled and centrifuged. The cell pellet was resuspended in DMEM (Gibco, Cat# C11995500BT) containing 10% FBS (Gibco, Cat# 10099141), 100 U/mL penicillin, and streptomycin (Gibco, Cat#15140122), and seeded for 4 hours at 37°C in a humidified 5% CO$_2$ incubator to separate cardiomyocytes and fibroblasts.

Dorsal root ganglia culture was executed according to literature[15]. Briefly, DRGs(T2-T6) were bilaterally dissected out from 5-8 days old C57BL/6 mice and digested for 45min at 37°C with DMEM/F12 based isolation medium containing 1 mg/mL type II Collagenase (40508ES60, Yeasen) and 2.5 mg/mL type II dispase (40104ES80, Yeasen). After digestion, cells were centrifuged and wash twice with a fresh culture medium and seeded in a 6-well plate in a 37°C incubator for 30min to remove glial cells. The supernatant was collected, centrifuged, and re-suspended with fresh DMEMF/12 containing 10%FBS, 1X glutamax, and 100ng/mL NGF (Gibco, 13257-019). For Ca2+ measurement, cells were seeded in 96-well plate and ready for experiment within 24 hours after isolation.

Surgery

Mice were anesthetized with isoflurane (RWD, Cat# R510-22) via an incubation tube. The depth of anesthesia was confirmed by a lack of flexor response to a toe pinch. Following sedation, mice were intubated and ventilated with 1% isoflurane mixed with room air (tidal volume 0.25 ml, 150 breaths per min) and placed on a heating pad. A left thoracotomy was to be made around the third intercostal space, where the beating heart was exposed. 5 nmol capsaicin (MCE, HY-10448) or 0.3nmol OB-Ala (Tocris, No.2142) or 0.3nmol OA or equal volume of saline was dropped on a 4mm2 filter paper and applied on the surface of the left ventricle. 30μmol OX1R specific antagonist SB334867 (MCE, HY-10895A) or OX2R specific antagonist EMPA (Sigma, SML0864) were applied on the heart surface 5min before the OA application and capsaicin. To induce acute myocardial infarction, the left anterior descendent coronary artery (LAD) was ligated with a 7-0 silk suture. Sham-operated mice underwent identical surgical procedures, except the LAD was not ligated. Saline or 0.3nmol OB-Ala was dropped on the filter paper and applied to the surface of the left ventricle immediately after LAD ligation. Regional infarction was confirmed by the pale color of the ligated area. Air was then evacuated from the chest, and the cavity was closed with respiration restored.

Echocardiography and Doppler imaging

The cardiac structure and function of mice subjected to LAD ligation were examined by echocardiography 24 hours after surgery with a high-resolution ultrasound system (Vevo 2100, Visual Sonics, Toronto, ON, Canada). Mice were anesthetized with 1% isoflurane in oxygen, and the depth of anesthesia was confirmed by a stable heart rate (400–500 bpm) and a lack of flexor response to a paw-pinch. Heart rate and other physiological parameters were continuously monitored by electrocardiogram (ECG) electrodes. A transducer (MS550D) was placed along the chest to obtain the parasternal long-axis images, and then the probe was rotated to acquire short-axis images at the level of the mid-papillary muscles. To obtain high-quality images, image acquisition was performed while avoiding excessive pressure over the sternum. All images were acquired and analyzed by the same blinded investigator according to the American Society of Echocardiography or calculated for three consecutive cardiac cycles and then averaged.

Intracerebroventricular injection

Mice were anesthetized using zoletil (50mg/kg, Virbac) mixed with xylazine hydrochloride (10mg/kg, MCE) and fixed on the stereotaxic instrument (RWD, 68002). The depth of anesthesia was confirmed by a lack of flexor response to a toe pinch. Cannulas were placed in the lateral ventricle with the coordination: +/− 1.2 (lateral), −0.6 (posterior), −2.2 (ventral) relative to Bregma. One week after surgery, mice received a 2uL single injection of vehicle or OB-Ala or OA as indicated in each experiment.

Measurement of HRV, arterial pressure and heart rate

Rat was anaesthetized with urethane (800 mg/kg) and chloralose (40 mg/kg). After endotracheal intubation, positive pressure ventilation was provided using a small animal ventilator (Model 683, Harvard Apparatus Inc., USA). To measure the arterial pressure and heart rate, a PE50 catheter was intubated into the right common carotid artery and connected to a pressure transducer (MLT0380, ADInstruments, Australia) and a data acquisition system (8SP, ADInstruments, Australia). To analyze the HRV, the electrocardiogram (ECG) was monitored with needle electrodes of standard II configuration embedded subcutaneously into the four extremities. The heart was exposed in the fourth intercostal space by bluntly dissecting the intercostal muscles. After surgical preparation was completed, the rat was stabilized for 30min before the experiments. Rats were divided into two groups: one group received epicardial vehicle treatment (corn oil) first, followed by capsaicin (5 nmol) 10min later; another group received epicardial OB-Ala (0.3nmol) treatment first, followed by capsaicin (5 nmol) 10 min later. The spectral power of HRV was evaluated from 2-minute ECG data after every intervention. The power spectral variables were defined as follows: low frequency component (LF) from 0.2 to 0.75 Hz, high frequency component (HF) from 0.75 to 2.5 Hz; and the ratio between LF and HF (LF/HF). The values are expressed as normalized units (nu). The change of MAP and HR was calculated as the difference between the maximum values within 2 min after every intervention and the mean value of baseline.

RTX injection

For sensory nerves denervation experiments, mice received subcutaneous injection of resiniferatoxin (RTX), a potent transient receptor vanilloid 1 (TRPV1) agonist, in three escalating doses for 3 consecutive days (30μg/kg, 70μg/kg, and 100μg/kg) as described in literature16. Mice were allowed to rest for 3 weeks before the epicardial capsaicin test.

Immunohistochemistry and immunofluorescence

Mice were anesthetized and perfused transcardially with cold PBS. The whole brain was fixed by 4% paraformaldehyde (PFA) for 48 h. The fixed brains were then dehydrated in 30% sucrose in PBS and then embedded with OCT (Sakura, Torrence, CA, USA) and cut into 30-μm-thick sections with a microtome. For DAB staining, brain slices were incubated with primary antibody overnight at 4°C and subsequently incubated with biotin-conjugated secondary antibody for 1 h at room temperature, followed by avidin-biotin-horseradish peroxidase complex. The reaction was visualized by 1% diaminobenzidine with 0.01% hydrogen peroxide and then counterstained with hematoxylin. Air-dried sections were dehydrated in alcohol gradient and 100% xylene. Slices were imaged with a fluorescence microscope (Olympus, Japan).

For immunofluorescent staining, hearts were embedded in paraffin and sectioned into 5-μm slices. Cultured cells on coverslips were fixed with 4% PFA. Samples were incubated with primary antibody overnight at 4°C, followed by Alex conjugated secondary antibody and mounted with antifading mounting medium with diamidino-2-phenylindole (DAPI). Confocal images were taken by LSM800 laser-scanning confocal microscope (Leica, Germany). The following primary antibodies were used: anti-c-Fos (9F6) (1:1000, Cell Signaling Technology, 2250T), anti-CRF (1:100, ImmunoStar, 20084), anti-Oxytocin (1:500, ImmunoStar, 20068), anti-cTnT (1:500, Abcam, AB8295), anti-CGRP (1:500, Abcam, ab81887). For CRF staining in PVN, 1uL of 0.1 μg/ml colchicine was injected into the lateral ventricles 24 hours before surgery.

Western blotting

Heart and brain tissues, or primary cells, underwent homogenization using RIPA lysis buffer supplemented with a protease inhibitor cocktail. After centrifugation, the protein concentration in the resulting supernatant was assessed using the BCA Protein Concentration Kit. Subsequently, the denatured protein samples were segregated on a 10% SDS-PAGE gel and subsequently transferred onto nitrocellulose membranes. These membranes were left to incubate overnight at 4°C with specific primary antibodies, including GAPDH (AF0911, Affinity) and OX2R (Ab183072, Abcam). The second day, the membranes were subjected to a two-hour incubation at room temperature with the

corresponding secondary antibodies. The protein bands were made visible using an ultrasensitive ECL reagent and then captured using the Bio-Rad automated gel imaging system.

RNAscope *in situ* hybridization

RNA *in situ* hybridization was performed with RNAscope Kit (RNAscope 2.5 HD Assay-Red, Advanced Cell Diagnostics) following the manufacturer's instructions. Briefly, mice were perfused with 4% PFA, and target organs were dissected out and post-fixed overnight at 4°C. After dehydration, samples were sectioned as 10 μm slices. After incubation with hydrogen peroxide and antigen retrieval, slices were digested with Protease Plus at 40°C for 30 min. Hcrtr2 probe (NM 198962.3) was used to detect Hcrtr2 mRNA *in situ*.

Intracellular Ca²⁺ flux assays

Primary DRG neurons and cardiomyocytes were prepared as described in the primary culture section. Intracellular Ca^{2+} flux was determined by Fluo-8 No Wash Calcium Assay kit (ab112129, Abcam). Cells were incubated with Fluo-8 for 30 min at 37°C in calcium-free Hanks' balanced salt solution (HHBS) and then brought to RT for another 30min. The drug was added as indicated. 10μM OX1R specific antagonist SB334867 (MCE, HY-10895A) or OX2R specific antagonist EMPA (Sigma, SML0864) were added 10min before OA and capsaicin. Fluorescence intensity was quantified at Ex/Em = 490/525 nm with a confocal microscope.

Measurement of cAMP

DRGs were isolated from T2-T6 immediately after sacrifice and frozen by liquid nitrogen. Tissues were homogenized with 100μL 0.1M HCl containing 0.5mM IBMX (Aladin, I106812) by sonication on ice. After centrifuge, the supernatant was neutralized with 0.72M KOH and assayed for cAMP concentration with an immunoassay kit (Cayman Chemical, 581001) according to the manufacturer's instructions.

Image analysis

For quantification of c-Fos staining, the c-Fos positive cells were quantified using a manual cell counter in ImageJ software. All images were minimally processed with threshold and contrast adjustment. Adjustments were applied uniformly throughout images and were consistent in the corresponding controls. Each coronal brain section was quantified by the average of the left side and the right side. Each brain sample was quantified by the average of two sections at the same anatomical level. The final number of positive cells reported was averaged from multiple images. Experimenters were blinded to treatments during imaging analysis.

QUANTIFICATION AND STATISTICAL ANALYSIS

Statistical analyses were performed using two-tailed unpaired t-tests and one-way analysis of variance (ANOVA) with GraphPad Prism 9 (San Diego, CA, USA). All data are presented as mean $\pm$ standard error of the mean (s.e.m.). $P<0.05$ was considered statistically significant.